

Spectral Element Discretization of the Stokes Equations in Deformed Axisymmetric Geometries

Zakaria Belhachmi^{1,*} and Andreas Karageorghis²

¹ *Laboratoire de Mathématiques, Informatique et Applications, EA CNRS, Université de Haute Alsace, Rue des Frères Lumières, 68096 Mulhouse, France*

² *Department of Mathematics and Statistics, University of Cyprus, P.O.Box 20537, 1678 Nicosia, Cyprus*

Received 27 August 2010; Accepted (in revised version) 28 January 2011

Available online 10 July 2011

Abstract. In this paper, we study the numerical solution of the Stokes system in deformed axisymmetric geometries. In the azimuthal direction the discretization is carried out by using truncated Fourier series, thus reducing the dimension of the problem. The resulting two-dimensional problems are discretized using the spectral element method which is based on the variational formulation in primitive variables. The meridian domain is subdivided into elements, in each of which the solution is approximated by truncated polynomial series. The results of numerical experiments for several geometries are presented.

AMS subject classifications: 65N35, 65N55

Key words: Spectral element method, Stokes equations, variational formulation, deformed geometries, Fourier expansion.

1 Introduction

In many problems of fluid mechanics one encounters flows in domains with axisymmetric geometries. Typical examples of such flows are the blood flow in vessels, hydrological problems (flow in pipelines), etc (see, e.g., [1] for more examples). As is well-documented [9], in axisymmetric geometries the solutions of the governing partial differential equations (PDEs) admit a Fourier expansion with respect to the angular (azimuthal) variable. The Fourier coefficients in this expansion are solutions of an infinite system of two-dimensional problems in the meridian domain. Such an expansion allows for a reduction of the dimension of the problem. In [2, 3] this idea

*Corresponding author.

URL: <http://www.math.uha.fr/belhachmi/>

Email: zakaria.belhachmi@uha.fr (Z. Belhachmi), andreak@ucy.ac.cy (A. Karageorghis)

was developed to derive an efficient strategy for solving the Stokes and Navier-Stokes equations with a finite element based discretization.

The extension of these ideas to spectral methods is non-trivial because of the complex nature of the meridian domains which, in this case, is a greater constraint in comparison to the finite element approach. In general, even after the decomposition of the meridian domain into simpler spectral elements, one has to deal with trapezoidal and curved sub-domains. In [15], it is shown that the spectral accuracy of spectral methods in such domains is preserved by applying the idea of *over-integration*. The aim of this paper is to combine this idea with a spectral element discretization to problems in *deformed* axisymmetric geometries, i.e., axisymmetric domains containing trapezoidal or curved parts. In particular, we study and develop a numerical procedure for solving the Stokes equations in deformed axisymmetric domains. This is achieved by the reduction of the dimension of the problem, where the full three-dimensional problem is replaced by an infinite system of two-dimensional problems, which, in turn, is approximated by a finite system of such problems. Each two-dimensional problem is solved with the spectral element method. We consider several geometries the discretization of which by spectral methods is non-trivial.

In particular, let Ω be a bounded connected domain in \mathbb{R}^3 , which is invariant under rotation around the z -axis. Also, assume that $\partial\Omega$ is the boundary of Ω . We consider the Stokes problem for an incompressible fluid

$$\begin{cases} -\Delta \mathbf{u} + \mathbf{grad} p = \mathbf{f}, & \text{in } \Omega, \\ \operatorname{div} \mathbf{u} = 0, & \text{in } \Omega, \\ \mathbf{u} = \mathbf{g}, & \text{on } \partial\Omega, \end{cases} \quad (1.1)$$

where \mathbf{u} is the velocity and p is the pressure of the fluid. In Problem (1.1), the external force \mathbf{f} and \mathbf{g} are given functions. We will further assume the usual flux condition

$$\int_{\partial\Omega} \mathbf{g} \cdot \mathbf{n} \, d\tau = 0, \quad (1.2)$$

where \mathbf{n} denotes the outward normal unit vector to $\partial\Omega$.

The paper is organized as follows. In Section 2 we introduce the Fourier expansion of Problem (1.1) and the functional (weighted) spaces necessary for the correct mathematical setting of the problem. We subsequently, provide the variational formulation for two-dimensional problems corresponding to the various Fourier modes. Section 3 is devoted to the spectral element discretization. In Section 4, we present the numerical procedure for the solution of the discrete problem. Finally, in Section 5 we present the results of several numerical experiments.

2 Variational formulation

2.1 Fourier expansion

Let (x, y, z) denote a set of Cartesian coordinates in \mathbb{R}^3 such that Ω is invariant under rotation around the z -axis. The polar coordinates (r, ϑ, z) , where $r \geq 0$ and $-\pi \leq \vartheta \leq$

π , are defined as usual by

$$x = r \cos \vartheta, \quad y = r \sin \vartheta \quad \text{and} \quad z = z,$$

and the domain Ω is generated by the rotation of the *meridian domain* ω around the z -axis, that is

$$\Omega = \{ (r, \vartheta, z); (r, z) \in \omega \text{ and } -\pi \leq \vartheta < \pi \}. \tag{2.1}$$

We will assume that ω is bounded, simply connected and has a Lipschitz-continuous boundary $\partial\omega$ consisting of two parts, namely γ_0 , which is the intersection of $\partial\omega$ with the axis $r = 0$, and γ which is $\partial\Omega \setminus \gamma_0$, that is

$$\gamma_0 \cap \gamma = \emptyset.$$

We further assume that γ_0 is the union of a finite number of straight segments and γ is the union of straight and possibly curved segments.

Following [9, Chapter X], the data f and g have the Fourier expansions

$$f(r, \vartheta, z) = \frac{1}{\sqrt{2\pi}} \sum_{k \in \mathbb{Z}} f^k(r, z) e^{ik\vartheta}, \quad g(r, \vartheta, z) = \frac{1}{\sqrt{2\pi}} \sum_{k \in \mathbb{Z}} g^k(r, z) e^{ik\vartheta}. \tag{2.2}$$

The vector fields

$$f = (f_r, f_\vartheta, f_z) \quad \text{and} \quad g = (g_r, g_\vartheta, g_z),$$

are said to be axisymmetric if all their Fourier coefficients in (2.2) are zero except the one of order $k = 0$. Similarly, the solution (u, p) can be written as

$$u(r, \vartheta, z) = \frac{1}{\sqrt{2\pi}} \sum_{k \in \mathbb{Z}} u^k(r, z) e^{ik\vartheta}, \quad p(r, \vartheta, z) = \frac{1}{\sqrt{2\pi}} \sum_{k \in \mathbb{Z}} p^k(r, z) e^{ik\vartheta}. \tag{2.3}$$

We thus have that (u, p) is a solution of Problem (1.1) if and only if each (u^k, p^k) , $k \in \mathbb{Z}$ is a solution of the two-dimensional problem [9, Chapter IX.1]

$$\left\{ \begin{array}{ll} -\partial_r^2 u_r^k - \frac{1}{r} \partial_r u_r^k - \partial_z^2 u_r^k + \frac{1+k^2}{r^2} u_r^k + \frac{2ik}{r} u_\vartheta^k + \partial_r p^k = f_r^k, & \text{in } \omega, \\ -\partial_r^2 u_\vartheta^k - \frac{1}{r} \partial_r u_\vartheta^k - \partial_z^2 u_\vartheta^k + \frac{1+k^2}{r^2} u_\vartheta^k - \frac{2ik}{r} u_r^k + \frac{ik}{r} p^k = f_\vartheta^k, & \text{in } \omega, \\ -\partial_r^2 u_z^k - \frac{1}{r} \partial_r u_z^k - \partial_z^2 u_z^k + \frac{k^2}{r^2} u_z^k + \partial_z p^k = f_z^k, & \text{in } \omega, \\ \partial_r u_r^k + \frac{1}{r} u_r^k + \frac{ik}{r} u_\vartheta^k + \partial_z u_z^k = 0, & \text{in } \omega, \\ (u_r, u_\vartheta, u_z) = (g_r, g_\vartheta, g_z), & \text{on } \gamma. \end{array} \right. \tag{2.4}$$

We will further assume that

$$\int_\gamma g^0 \cdot n \, d\tau = 0. \tag{2.5}$$

Moreover, if the data (f, g) are axisymmetric, so is the solution (u, p) , in the sense that (u_r, u_ϑ, u_z) and p are independent of ϑ .

In order to write the variational formulation of Problem (2.4), we introduce the weighted spaces

$$L^2_{\pm 1}(\omega) = \left\{ v : \omega \leftarrow \mathbb{C}, \text{ measurable; } \int_{\omega} |v(r, z)|^2 r^{\pm 1} dr dz < +\infty \right\}, \quad (2.6)$$

equipped with the norms

$$\|v\|_{L^2_{\pm 1}(\omega)} = \left(\int_{\omega} |v(r, z)|^2 r^{\pm 1} dr dz \right)^{\frac{1}{2}}.$$

The complete Sobolev scale $H^s_1(\omega)$, $s \in \mathbb{R}$ is defined in a standard way [14], namely, when s is an integer, $H^s_1(\omega)$ is the space of functions of $L^2_1(\omega)$ such that all their partial derivatives of order $\leq s$ belong to $L^2_1(\omega)$ while when s is not an integer $H^s_1(\omega)$ is defined by Hilbertian interpolation. Note that when s is an integer, $H^s_1(\omega)$ is equipped with the following semi-norm and norm

$$|v|_{H^s_1(\omega)} = \left(\sum_{\ell=0}^s \|\partial_r^\ell \partial_z^{s-\ell} v\|_{L^2_1(\omega)}^2 \right)^{\frac{1}{2}} \quad \text{and} \quad \|v\|_{H^s_1(\omega)} = \left(\sum_{k=0}^s |v|_{H^k_1(\omega)}^2 \right)^{\frac{1}{2}},$$

respectively.

We also introduce the space

$$V^1_1(\omega) = H^1_1(\omega) \cap L^2_{-1}(\omega), \quad (2.7)$$

equipped with the norm

$$\|v\|_{V^1_1(\omega)} = \left(\|v\|_{L^2_{-1}(\omega)}^2 + |v|_{H^1_1(\omega)}^2 \right)^{\frac{1}{2}},$$

and the variational spaces

$$L^2_{1,0}(\omega) = \left\{ q \in L^2_1(\omega); \int_{\omega} q(r, z) r dr dz = 0 \right\}, \quad (2.8)$$

and

$$H^1_{1\circ}(\omega) = \{v \in H^1_1(\omega); v = 0, \text{ on } \gamma\}. \quad (2.9)$$

Finally, for each mode k we define the space (associated with mode k)

$$\mathbf{H}^1_k = \begin{cases} V^1_1(\omega) \times V^1_1(\omega) \times H^1_1(\omega), & \text{if } k = 0, \\ \{(v_r, v_\theta, v_z) \in H^1_1(\omega) \times H^1_1(\omega) \times V^1_1(\omega), v_r + ikv_\theta \in L^2_{-1}(\omega)\}, & \text{if } |k| = 1, \\ V^1_1(\omega) \times V^1_1(\omega) \times V^1_1(\omega), & \text{if } |k| \geq 2, \end{cases} \quad (2.10)$$

and its corresponding subspace

$$\mathbf{H}^1_{k\circ}(\omega) = \mathbf{H}^1_k(\omega) \cap H^1_{1\circ}(\omega)^3. \quad (2.11)$$

By defining

$$a_k(u, v) = \int_{\omega} (\partial_r u \partial_r \bar{v} + \partial_z u \partial_z \bar{v})(r, z) r dr dz + k^2 \int_{\omega} u(r, z) \bar{v}(r, z) r^{-1} dr dz,$$

we next introduce the sesquilinear forms for each k

$$\begin{aligned} \mathcal{A}_k(\mathbf{u}, \mathbf{v}) &= a_0(u_r, v_r) + a_0(u_{\vartheta}, v_{\vartheta}) + a_0(u_z, v_z) + \int_{\omega} \left((1 + k^2) (u_r \bar{v}_r + u_{\vartheta} \bar{v}_{\vartheta}) \right. \\ &\quad \left. + \frac{2ik}{r} (u_{\vartheta} \bar{v}_r - u_r \bar{v}_{\vartheta}) + k^2 u_z \bar{v}_z \right) (r, z) r^{-1} dr dz, \\ \mathcal{B}_k(\mathbf{v}, q) &= - \int_{\omega} q(r, z) (\partial_r \bar{v}_r + r^{-1} \bar{v}_r + ikr^{-1} \bar{v}_{\vartheta} + \partial_z \bar{v}_z) (r, z) r dr dz. \end{aligned}$$

For simplicity, we denote by $L_k^2(\omega)$ the space $L_0^2(\omega)$ for $k = 0$ and $L_1^2(\omega)$ for $k \neq 0$.

Following [9, Chapter IX], the variational formulation of Problem (2.4) is: find (\mathbf{u}^k, p^k) in $\mathbf{H}_k^1(\omega) \times L_k^2(\omega)$, with \mathbf{u}^k equal to \mathbf{g}^k on γ , such that

$$\begin{cases} \forall \mathbf{v} \in \mathbf{H}_{k,\diamond}^1(\omega), & \mathcal{A}_k(\mathbf{u}^k, \mathbf{v}) + \mathcal{B}_k(\mathbf{v}, p^k) = \int_{\omega} (\mathbf{f}^k \cdot \bar{\mathbf{v}}) (r, z) r dr dz, \\ \forall q \in L_k^2(\omega), & \bar{\mathcal{B}}_k(\mathbf{u}^k, q) = 0. \end{cases} \quad (2.12)$$

For each k , we introduce the norm associated with $\mathbf{H}_k^1(\omega)$,

$$\|\mathbf{v}\|_{\mathbf{H}_k^1(\omega)} = \mathcal{A}_k(\mathbf{v}, \mathbf{v})^{\frac{1}{2}}.$$

This norm is equivalent to the norm $\|\mathbf{v} e^{ik\vartheta}\|_{H^1(\Omega)^3}$, with equivalence constants independent of k . As a consequence, we easily derive the following inf-sup condition from its analogue on Ω , namely, there exists a positive constant β such that, for all $k \in \mathbb{Z}$,

$$\forall q \in L_k^2(\omega), \quad \sup_{\mathbf{v} \in \mathbf{H}_k^1(\omega)} \frac{\mathcal{B}_k(\mathbf{v}, q)}{\|\mathbf{v}\|_{\mathbf{H}_k^1(\omega)}} \geq \beta \|q\|_{L_1^2(\omega)}.$$

If we assume that the data \mathbf{f}^k belong to the dual space of $\mathbf{H}_{k,\diamond}^1(\omega)$ and that the function \mathbf{g}^k admits a lifting $\bar{\mathbf{g}}^k$ in $\mathbf{H}_k^1(\omega)$ and satisfies (2.7) if k is equal to zero, then Problem (2.12) has a unique solution (\mathbf{u}^k, p^k) in $\mathbf{H}_k^1(\omega)$. Moreover this solution satisfies the inequality

$$\|\mathbf{u}^k\|_{\mathbf{H}_k^1(\omega)} + \|p^k\|_{L_1^2(\omega)} \leq c (\|\mathbf{f}^k\|_{\mathbf{H}_{k,\diamond}^1(\omega)'} + \|\bar{\mathbf{g}}^k\|_{\mathbf{H}_k^1(\omega)}). \quad (2.13)$$

2.2 Reduction of dimension

The reduction of dimension results from the Fourier truncation of the infinite system of Eq. (2.12).

Since, in general, the data \mathbf{f} and \mathbf{g} cannot be computed explicitly, we introduce the nodes

$$\vartheta_m = \frac{2m\pi}{2K+1}, \quad -K \leq m \leq K,$$

where K is an integer ≥ 2 . We also define the approximate Fourier coefficients for $-K \leq k \leq K$ as

$$f_*^k(r, z) = \frac{\sqrt{2\pi}}{2K+1} \sum_{m=-K}^K f(r, \vartheta_m, z) e^{-ik\vartheta_m}, \tag{2.14a}$$

$$g_*^k(r, z) = \frac{\sqrt{2\pi}}{2K+1} \sum_{m=-K}^K g(r, \vartheta_m, z) e^{-ik\vartheta_m}. \tag{2.14b}$$

The System (cf. (2.12)) now becomes: for $-K \leq k \leq K$,

$$\left\{ \begin{array}{l} \text{find } (\mathbf{u}_*^k, p_*^k) \in \mathbf{H}_k^1(\omega) \times L_k^2(\omega), \text{ such that} \\ \mathbf{u}_*^k = \mathbf{g}_*^k, \text{ on } \gamma, \text{ and} \\ \forall v \in \mathbf{H}_{k,\diamond}^1(\omega), \quad \mathcal{A}_k(\mathbf{u}_*^k, v) + \mathcal{B}_k(v, p_*^k) = \int_{\omega} (\mathbf{f}_*^k \cdot \bar{v})(r, z) r dr dz, \\ \forall q \in L_k^2(\omega), \quad \bar{\mathcal{B}}^k(\mathbf{u}_*^k, q) = 0. \end{array} \right. \tag{2.15}$$

The reconstruction formula for the three-dimensional solution (\mathbf{u}_K, p_K) associated with the solution of System (2.15) is given by

$$\mathbf{u}_K(r, \vartheta, z) = \frac{1}{\sqrt{2\pi}} \sum_{k=-K}^K \mathbf{u}_*^k(r, z) e^{ik\vartheta}, \quad p_K(r, \vartheta, z) = \frac{1}{\sqrt{2\pi}} \sum_{k=-K}^K p_*^k(r, z) e^{ik\vartheta}. \tag{2.16}$$

If we define

$$H^{m,\sigma}(\Omega) = \{v \in H^m(\Omega); \partial_{\vartheta}^{\ell} v \in H^m(\Omega), 1 \leq \ell \leq \sigma\},$$

in the case σ is a nonnegative integer and by Hilbertian interpolation otherwise, the following result [9, Theorem IX 2.23], holds,

Proposition 2.1. *Assume that the data $\mathbf{f} \in H^{-1,\sigma}(\Omega)^3$, for a real number $\sigma > 0$, and \mathbf{g} admits a lifting, also denoted by \mathbf{g} , in $H^{1,\sigma}(\Omega)^3$. Then the following error estimate holds*

$$\|\mathbf{u} - \mathbf{u}_K\|_{H^1(\Omega)^3} + \|p - p_K\|_{L^2(\Omega)} \leq cK^{-\sigma} (\|\mathbf{f}\|_{H^{-1,\sigma}(\Omega)^3} + \|\mathbf{g}\|_{H^{1,\sigma}(\Omega)^3}). \tag{2.17}$$

From Proposition 2.1, it follows that for sufficiently smooth data, only a few modes are required to compute an accurate approximation to the solution of the initial problem.

3 Spectral element discretization

Given a partition of the meridian domain ω without overlap

$$\bar{\omega} = \cup_{\ell=1}^L \bar{\omega}_{\ell} \quad \text{and} \quad \omega_{\ell} \cap \omega_{\ell'} = \emptyset, \quad 1 \leq \ell < \ell' \leq L,$$

we will assume that the intersection of $\partial\omega_\ell$ and $\partial\omega_{\ell'}$, $1 \leq \ell < \ell' \leq L$, if not empty, is a vertex or a whole edge of both ω_ℓ and $\omega_{\ell'}$. In addition, the intersection of each $\partial\omega_\ell$, $1 \leq \ell \leq L$, with γ_0 , if not empty, is a whole edge of both ω_ℓ and $\omega_{\ell'}$.

We are interested in sub-domains which are either *rectangular or trapezoidal elements*, or *curvilinear elements*.

In both cases, we will assume there exists a one-to-one mapping F_ℓ from the reference square $\hat{\omega} = [-1, 1]^2$ onto ω_ℓ such that both F_ℓ and F_ℓ^{-1} are infinitely differentiable, for each sub-domain ω_ℓ , $1 \leq \ell \leq L$. The images of the vertices of $\hat{\omega}$ via F_ℓ are called vertices of ω_ℓ and the images of the edges of $\hat{\omega}$ via F_ℓ are called edges of ω_ℓ . We set

$$\delta = (N, N_\#),$$

to be a pair of integers ≥ 2 . For each integer $n \geq 0$, we denote by $\mathbb{P}_n(\hat{\omega})$ the space of restrictions to $\hat{\omega}$ of polynomials in two variables and degree $\leq n$ with respect to each variable.

We define the basic discrete spaces as follows

$$\mathbf{X}_\delta^{(k)} = \left\{ \mathbf{v}_\delta \in \mathbf{H}_{(k)}^1(\omega); \mathbf{v}_{\delta|\omega_\ell} \circ F_\ell \in \mathbb{P}_N(\hat{\omega}), 1 \leq \ell \leq L \right\}, \tag{3.1a}$$

$$M_\delta^{(k)} = \left\{ q_\delta \in L_{(k)}^2(\omega); q_{\delta|\omega_\ell} \circ F_\ell \in \mathbb{P}_{N-2}(\hat{\omega}), 1 \leq \ell \leq L \right\}, \tag{3.1b}$$

and also introduce the discrete variational spaces

$$\mathbf{X}_\delta^{(k)\diamond}(\omega) = \mathbf{X}_\delta^{(k)} \cap H_{1^\diamond}^1(\omega)^3. \tag{3.2}$$

We recall the main properties of the Gauss-Lobatto quadrature formula. For each positive integer n , with $\xi_0 = -1$ and $\xi_n = 1$, there exist a unique set of nodes ξ_j , $1 \leq j \leq n - 1$, in $[-1, 1]$ and a unique set of weights ρ_j , $0 \leq j \leq n$, such that

$$\forall \Phi \in \mathbb{P}_{2n-1}(-1, 1), \quad \int_{-1}^1 \Phi(\zeta) d\zeta = \sum_{j=0}^n \Phi(\xi_j) \rho_j. \tag{3.3}$$

Moreover, the following positivity property holds (see, [11, Eq. (13.20)]):

$$\forall \varphi_n \in \mathbb{P}_n(-1, 1), \quad \|\varphi_n\|_{L^2(-1,1)}^2 \leq \sum_{j=0}^n \varphi_n^2(\xi_j) \rho_j \leq 3 \|\varphi_n\|_{L^2(-1,1)}^2.$$

Next, taking $n = N_\#$, and in view of the integration formula

$$\int_{\omega_\ell} u(r, z) \bar{v}(r, z) r dr dz = \int_{\hat{\omega}} (u \circ F_\ell)(\zeta, \xi) (\bar{v} \circ F_\ell)(\zeta, \xi) R_\ell(\zeta, \xi) J_\ell(\zeta, \xi) d\zeta d\xi,$$

where R_ℓ is the first component of the mapping F_ℓ and J_ℓ the absolute value of its Jacobian, we define the discrete product, for all functions u and v continuous on $\bar{\omega}_\ell$, by

$$(u, v)_\ell = \sum_{i=0}^{N_\#} \sum_{j=0}^{N_\#} (u \circ F_\ell)(\xi_i^\ell, \xi_j^\ell) (\bar{v} \circ F_\ell)(\xi_i^\ell, \xi_j^\ell) R_\ell(\xi_i^\ell, \xi_j^\ell) J_\ell(\xi_i^\ell, \xi_j^\ell) \rho_i^\ell \rho_j^\ell. \tag{3.4}$$

The global product is then defined by

$$[u, v]_\delta = \sum_{\ell=1}^L (u, v)_\ell. \tag{3.5}$$

Remark 3.1. When ω_ℓ is the rectangle $[r_1, r_2] \times [z_1, z_2]$, F_ℓ is affine and given by

$$F_\ell(\zeta, \xi) = \begin{pmatrix} r_1 + \frac{r_2-r_1}{2}(1 + \zeta) \\ z_1 + \frac{z_2-z_1}{2}(1 + \xi) \end{pmatrix},$$

and its Jacobian matrix is diagonal. In this case, (3.4) becomes the usual formula

$$(u, v)_\ell = \frac{(r_2 - r_1)(z_2 - z_1)}{4} \sum_{i=0}^{N_\#} \sum_{j=0}^{N_\#} u(r_i^\ell, z_j^\ell) \bar{v}(r_i^\ell, z_j^\ell) r_i^\ell \rho_i^\ell \rho_j^\ell.$$

The use of over-integration is only required for curved elements (and in the direction of the curved edges), thus the parameter $N_\# > N$ in the formula (3.4) could be replaced by N when over integration is not necessary.

The discrete sesquilinear forms are now defined by

$$\begin{aligned} \mathcal{A}_{k\delta}(\mathbf{u}, \mathbf{v}) &= a_{0\delta}(u_r, v_r) + a_{0\delta}(u_\theta, v_\theta) + a_{0\delta}(u_z, v_z) + (1 + k^2) \\ &\quad + (1 + k^2) [u_\theta r^{-1}, v_\theta r^{-1}]_\delta + 2ik [u_\theta r^{-1}, v_r r^{-1}]_\delta \\ &\quad - 2ik [u_r r^{-1}, v_\theta r^{-1}]_\delta + k^2 [u_z r^{-1}, v_z r^{-1}]_\delta, \end{aligned} \tag{3.6a}$$

$$\mathcal{B}_{k\delta}(\mathbf{v}, q) = -[q, (\partial_r \bar{v}_r + r^{-1} \bar{v}_r + ikr^{-1} \bar{v}_\theta + \partial_z \bar{v}_z)]_\delta, \tag{3.6b}$$

where

$$a_{0\delta}(u, v) = [\partial_r u, \partial_r v]_\delta + [\partial_z u, \partial_z v]_\delta. \tag{3.7}$$

If we let \mathcal{I}_N denote the Lagrange interpolation operator at all nodes (r_i, z_j) , $1 \leq i, j \leq N$ and for each k still denote by \mathbf{g}_*^k a lifting of the data \mathbf{g}_*^k to ω , then the discrete problem associated with (2.15) reads:

$$\left\{ \begin{array}{l} \text{For each } -K \leq k \leq K, \text{ find } (\mathbf{u}_\delta^k, p_\delta^k) \in \mathbf{X}_\delta^k(\omega) \times M_\delta^k(\omega), \text{ such that} \\ \mathbf{u}_\delta^k = \mathcal{I}_N \mathbf{g}_*^k, \text{ on } \gamma, \text{ and} \\ \forall \mathbf{v}_\delta \in \mathbf{X}_\delta^{k,\diamond}(\omega), \mathcal{A}_{k\delta}(\mathbf{u}_\delta^k, \mathbf{v}_\delta) + \mathcal{B}_{k\delta}(\mathbf{v}_\delta, p_\delta^k) = \int_\omega (\mathcal{I}_N \mathbf{f}_*^k \cdot \bar{\mathbf{v}}_\delta)(r, z) r dr dz, \\ \forall q_\delta \in M_\delta^k(\omega), \bar{\mathcal{B}}_k(\mathbf{u}_\delta^k, q_\delta) = 0. \end{array} \right. \tag{3.8}$$

Combining the arguments of [15] and [5], it can be verified that under the condition

$$N_\# > N, \tag{3.9}$$

the sesquilinear forms $A_k(\cdot, \cdot)$ and $B_k(\cdot, \cdot)$ are continuous and that the inf-sup condition is satisfied which yields the well-posedness of Problem (3.8).

4 Numerical implementation

In the implementation of the method we shall use the saddle-point approach proposed in [8] (see also [6] for more specific details) which is equivalent to Problem (3.8). To this end, let us briefly describe the discrete saddle-point formulation. We denote by S the skeleton of the decomposition of ω which is equal to $\bigcup_{\ell=1}^L \partial\omega_\ell \setminus \partial\omega$. The skeleton S can also be defined as a union of disjoint open edges (mortars),

$$\bar{S} = \bigcup_{m=1}^{M^*} \bar{\gamma}_m, \quad \gamma_m \cap \gamma_{m'} = \emptyset, \quad 1 \leq m < m' \leq M^*, \tag{4.1}$$

where each γ_m is a whole edge of one of the ω_ℓ , denoted by $\omega_{\ell(m)}$.

We introduce the space T_δ as

$$T_\delta = \prod_{m=1}^{M^*} P_{N-2}(\gamma_m)^3,$$

and define the sesquilinear form $\mathcal{D}_{\delta k}(\cdot, \cdot)$ on $X_\delta^k(\omega) \times T_\delta$ by

$$\mathcal{D}_{\delta k}(\mathbf{v}_\delta^k, \mu_\delta) = \sum_{m=1}^{M^*} \int_{\gamma_m} [\mathbf{v}_\delta] \cdot \mu_\delta \, d\tau. \tag{4.2}$$

Note that from the definition of T_δ , the integrals which appear in (4.2) can be equivalently replaced by the Gauss-Lobatto quadrature formula at the nodes ξ_j , which belong to γ_m .

Thus Problem (3.8) may be written in the equivalent form:

$$\left\{ \begin{array}{l} \text{For each } -K \leq k \leq K, \text{ find} \\ (\mathbf{u}_\delta^k, p_\delta^k) \in X_\delta^k(\omega) \times M_\delta^k(\omega) \text{ and } \lambda_\delta = (\lambda_{\delta,r}, \lambda_{\delta,\theta}, \lambda_{\delta,z}) \in T_\delta, \text{ such that} \\ \mathbf{u}_\delta^k = \mathcal{I}_N \mathbf{g}_*^k, \text{ on } \gamma, \text{ and} \\ \forall \mathbf{v}_\delta \in X_\delta^{k,\circ}(\omega), \mathcal{A}_{k\delta}(\mathbf{u}_\delta^k, \mathbf{v}_\delta) + \mathcal{B}_{k\delta}(\mathbf{v}_\delta, p_\delta^k) + \mathcal{D}_{k\delta}(\mathbf{v}_\delta, \lambda_\delta) = \int_\omega (\mathcal{I}_N \mathbf{f}_*^k \cdot \bar{\mathbf{v}}_\delta)(r, z) r dr dz, \\ \forall q_\delta \in M_\delta^k(\omega), \bar{\mathcal{B}}_k(\mathbf{u}_\delta^k, q_\delta) = 0, \\ \forall \mu_\delta \in T_\delta, \bar{\mathcal{D}}_{\delta k}(\mathbf{u}_\delta^k, \mu_\delta) = 0. \end{array} \right. \tag{4.3}$$

It may be readily verified that if $(\mathbf{u}_\delta^k, p_\delta^k, \lambda_\delta)$, $-K \leq k \leq K$ is a solution of Problem (4.3), then $(\mathbf{u}_\delta^k, p_\delta^k)$, $-K \leq k \leq K$ is also solution of Problem (3.8). Conversely, it can be proved as in [8] that the only spurious mode μ_δ in T_δ satisfying

$$\forall \mathbf{v}_\delta \in X_\delta^k, \quad \mathcal{D}_{\delta k}(\mathbf{v}_\delta, \mu_\delta) = 0,$$

is zero, and therefore Problem (4.3) is well-posed.

In all examples considered the meridian domain ω is subdivided into three elements such that

$$\omega = \omega_I \cup \omega_{II} \cup \omega_{III}.$$

Further, the boundary $\partial\omega$ of ω , as mentioned in Section 2.1, is written as

$$\partial\omega = \gamma_0 \cup \gamma.$$

In the examples considered, we take

$$\gamma = \gamma_i \cup \gamma_o,$$

where $\gamma_i = [0, r_i] \times z_i$ and $\gamma_o = [0, r_o] \times z_o$, that is the domain ω lies between the two vertical lines $z = z_i$ and $z = z_o$, see [2]. In all numerical examples we shall assume that g_r and g_θ vanish on γ and that g_z vanishes on $\gamma \setminus (\gamma_i \cup \gamma_o)$. We also assume that

$$f = \mathbf{0}.$$

We next present the main features of the implementational process. For the sake of brevity the full details of the implementation of the method are omitted and may be found in [7].

For each k , we approximate the solution $((u_r, u_\theta, u_z), p)$ in each of the three elements as follows (note that $\zeta, \eta \in [-1, 1]$ and that $(r, z) \rightarrow (\zeta, \xi)$):

$$u_{r_\ell}^k(\zeta, \xi) = \sum_{i=0}^N \sum_{j=0}^N u_{r_{\ell ij}}^k q_i(\zeta) q_j(\xi), \quad u_{\theta_\ell}^k(\zeta, \xi) = \sum_{i=0}^N \sum_{j=0}^N u_{\theta_{\ell ij}}^k q_i(\zeta) q_j(\xi), \quad (4.4a)$$

$$u_{z_\ell}^k(\zeta, \xi) = \sum_{i=0}^N \sum_{j=0}^N u_{z_{\ell ij}}^k q_i(\zeta) q_j(\xi), \quad p_\ell^k(\zeta, \xi) = \sum_{i=0}^{N-2} \sum_{j=0}^{N-2} p_{\ell ij}^k L_i(\zeta) L_j(\xi), \quad (4.4b)$$

with $\ell = I, II, III$. In (4.4), $\{L_n(\xi)\}_{n=1}^\infty$, $\xi \in [-1, 1]$ is the set of Legendre polynomials, the q_i are the Lagrange interpolating polynomials for the set of points $\{\xi_j\}_{j=0}^N$ which are the nodes of the Gauss-Lobatto quadrature formula (3.3). Further details regarding the derivation of the Lagrange interpolating polynomials are provided in the Appendix.

Problem (4.3) yields a system of the form

$$\left(\begin{array}{c|c|c} A & D & B \\ \hline D^T & 0 & 0 \\ \hline \overline{B}^T & 0 & 0 \end{array} \right) \begin{pmatrix} \mathbf{u} \\ \boldsymbol{\lambda} \\ \mathbf{p} \end{pmatrix} = \begin{pmatrix} \mathcal{F} \\ \mathbf{0} \\ \mathcal{G} \end{pmatrix}, \quad (4.5)$$

where vectors \mathbf{u} , \mathbf{p} and $\boldsymbol{\lambda}$ will have the form

$$\mathbf{u} = \begin{pmatrix} \mathbf{u}_{r_I}^k \\ \mathbf{u}_{\theta_I}^k \\ \mathbf{u}_{z_I}^k \\ \mathbf{u}_{r_{II}}^k \\ \mathbf{u}_{\theta_{II}}^k \\ \mathbf{u}_{z_{II}}^k \\ \mathbf{u}_{r_{III}}^k \\ \mathbf{u}_{\theta_{III}}^k \\ \mathbf{u}_{z_{III}}^k \end{pmatrix}, \quad \mathbf{p} = \begin{pmatrix} \mathbf{p}_I^k \\ \mathbf{p}_{II}^k \\ \mathbf{p}_{III}^k \end{pmatrix}, \quad \boldsymbol{\lambda} = \begin{pmatrix} \boldsymbol{\lambda}_{r_{I,II}}^k \\ \boldsymbol{\lambda}_{\theta_{I,II}}^k \\ \boldsymbol{\lambda}_{z_{I,II}}^k \\ \boldsymbol{\lambda}_{r_{II,III}}^k \\ \boldsymbol{\lambda}_{\theta_{II,III}}^k \\ \boldsymbol{\lambda}_{z_{II,III}}^k \end{pmatrix},$$

respectively.

After taking into account the boundary conditions for \mathbf{u} , the unknowns to be determined in each element and the interfaces are:

$$\begin{aligned} \omega_I & \left\{ u_{r_{ij}}^k \right\}_{i=1,j=1}^{N-1,N}, \left\{ u_{\theta_{ij}}^k \right\}_{i=1,j=1}^{N-1,N}, \left\{ u_{z_{ij}}^k \right\}_{i=0,j=1}^{N-1,N}, \left\{ p_{ij}^k \right\}_{i=0,j=0}^{N-2,N-2} . \\ \omega_{II} & \left\{ u_{r_{ij}}^k \right\}_{i=1,j=0}^{N,N-1}, \left\{ u_{\theta_{ij}}^k \right\}_{i=1,j=0}^{N,N-1}, \left\{ u_{z_{ij}}^k \right\}_{i=0,j=0}^{N,N-1}, \left\{ p_{ij}^k \right\}_{i=0,j=0}^{N-2,N-2} . \\ \omega_{III} & \left\{ u_{r_{ij}}^k \right\}_{i=0,j=1}^{N-1,N-1}, \left\{ u_{\theta_{ij}}^k \right\}_{i=0,j=1}^{N-1,N-1}, \left\{ u_{z_{ij}}^k \right\}_{i=0,j=1}^{N-1,N-1}, \left\{ p_{ij}^k \right\}_{i=0,j=0}^{N-2,N-2} . \\ \text{Interface } I - II & \left\{ \lambda_{r_{I,II_i}}^k \right\}_{i=1}^{N-1}, \left\{ \lambda_{\theta_{I,II_i}}^k \right\}_{i=1}^{N-1}, \left\{ \lambda_{z_{I,II_i}}^k \right\}_{i=1}^{N-1} . \\ \text{Interface } II - III & \left\{ \lambda_{r_{II,III_i}}^k \right\}_{i=1}^{N-1}, \left\{ \lambda_{\theta_{II,III_i}}^k \right\}_{i=1}^{N-1}, \left\{ \lambda_{z_{II,III_i}}^k \right\}_{i=1}^{N-1} . \end{aligned}$$

From the expressions (3.6)-(3.6b), the submatrices of the matrices A and B in (4.6a) and (4.6c) correspond to the discrete products:

$$A_\ell^r : a_{0\delta}(u_r, v_r) + (1 + k^2)[u_r r^{-1}, v_r r^{-1}]_\delta, \quad A_\ell^{r\theta} : 2ik[u_\theta r^{-1}, v_r r^{-1}]_\delta, \quad (4.7a)$$

$$A_\ell^\theta : a_{0\delta}(u_\theta, v_\theta) + (1 + k^2)[u_\theta r^{-1}, v_\theta r^{-1}]_\delta, \quad A_\ell^{\theta r} : -2ik[u_r r^{-1}, v_\theta r^{-1}]_\delta, \quad (4.7b)$$

$$A_\ell^z : a_{0\delta}(u_z, v_z) + k^2[u_z r^{-1}, v_z r^{-1}]_\delta, \quad B_\ell^r : -[p, \partial_r v_r + r^{-1} v_r]_\delta, \quad (4.7c)$$

$$B_\ell^\theta : -ik[p, r^{-1} u_\theta]_\delta, \quad B_\ell^z : -[p, \partial_z v_z]_\delta, \quad (4.7d)$$

for $\ell = I, II, III$.

The submatrices of D in (4.6b) will have all but a few zero elements. The non-zero elements will be either 1 or -1 ensuring the continuity of the approximations at the nodes across the interfaces.

The entries of the vectors \mathcal{F} and \mathcal{G} come from the non-zero boundary conditions for u_z on γ_i and γ_o .

After the incorporation of the boundary conditions, the sizes of the submatrices and subvectors in System (4.5) are as follows:

- The matrices $A_I^r, A_I^{r\theta}, A_I^{\theta r}, A_I^\theta$ will all have size $N(N - 1) \times N(N - 1)$ and the matrix A_I^z will have size $N^2 \times N^2$.
- The matrices $A_{II}^r, A_{II}^{r\theta}, A_{II}^{\theta r}, A_{II}^\theta$ will all have size $N^2 \times N^2$ and the matrix A_{II}^z will have size $N(N + 1) \times N(N + 1)$.
- The matrices $A_{III}^r, A_{III}^{r\theta}, A_{III}^{\theta r}, A_{III}^\theta, A_{III}^z$ will all have size $N(N - 1) \times N(N - 1)$.
- The matrices B_I^r, B_I^θ will both have size $N(N - 1) \times (N - 1)^2$ and the matrix B_I^z will have size $N^2 \times (N - 1)^2$.
- The matrices B_{II}^r, B_{II}^θ will both have size $N^2 \times (N - 1)^2$ and the matrix B_{II}^z will have size $N(N + 1) \times (N - 1)^2$.
- The matrices $B_{III}^r, B_{III}^\theta, B_{III}^z$ will all have size $N(N - 1) \times (N - 1)^2$.

- The matrices $D_{I,II}^r$, $D_{I,II}^\theta$ will both have size $N(N-1) \times (N-1)$ and the matrix $D_{I,II}^z$ will have size $N^2 \times N$.
- The matrices $D_{II,I}^r$, $D_{II,I}^\theta$ will both have size $N^2 \times (N-1)$ and the matrix $D_{II,I}^z$ will have size $N(N+1) \times N$.
- The matrices $D_{II,III}^r$, $D_{II,III}^\theta$ will both have size $N^2 \times (N-1)$ and the matrix $D_{II,III}^z$ will have size $N(N+1) \times (N-1)$.
- The matrices $D_{III,II}^r$, $D_{III,II}^\theta$, $D_{III,II}^z$ will all have size $N(N-1) \times (N-1)$.
- The vectors \mathcal{F}_I^z , \mathcal{F}_{II}^z , \mathcal{F}_{III}^z will have size $N^2 \times 1$, $N(N+1) \times 1$, $N(N-1) \times 1$, respectively. The vectors \mathcal{G}_I , \mathcal{G}_{II} , \mathcal{G}_{III} , will all have size $(N-1)^2 \times 1$.

5 Numerical examples

In the axisymmetric case ($k = 0$) considered, the boundary conditions are defined by (see, [2])

$$\begin{aligned} g_z(r, -2) &= 4(1 - r^2), & \text{on } \gamma_i, \\ g_z(r, 2) &= \frac{1}{4}(4 - r^2), & \text{on } \gamma_e, \end{aligned}$$

while in the case $k = 3$, also considered, the boundary conditions defined by (see, [2])

$$\begin{aligned} g_z(r, -2) &= 4r^2(1 - r^2) \sin(3\theta), & \text{on } \gamma_i, \\ g_z(r, 2) &= \frac{1}{4}r^2(4 - r^2) \cos(3\theta), & \text{on } \gamma_e. \end{aligned}$$

5.1 Example 1

We consider the rectangularly decomposable domain depicted in Fig. 1, defined by

$$\omega_I = [0, 1] \times [-2, 0], \quad \omega_{II} = [0, 1] \times [0, 2], \quad \omega_{III} = [1, 2] \times [0, 2].$$

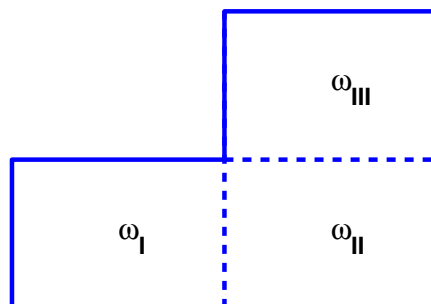


Figure 1: Geometry for Example 1.

5.1.1 Case $k = 0$

In Figs. 2(a) and 2(b), we present the isolines of the coordinates u_z and u_r of the velocity, respectively, for $N = 28$. These results are in excellent agreement with the corresponding results of [2]. We have also observed the consistency of the results for different numbers of degrees of freedom and for N as little as 12 the results are almost indistinguishable.

We also calculated the values of u_z and u_r on a uniform 51×51 grid in each of the three elements for $N = 8, 12, 16, 20, 24, 28$ and 30. We subsequently calculated the quantities $\|u_{z_N} - u_{z_{30}}\|_\infty, \|u_{r_N} - u_{r_{30}}\|_\infty, N = 8, 12, 16, 20, 24, 28$, to be the maximum absolute difference at these points. In Fig. 3, we present the log-log plots for $\|u_{z_N} - u_{z_{30}}\|_\infty$ and $\|u_{r_N} - u_{r_{30}}\|_\infty$ versus N . Both plots in Fig. 3 exhibit spectral accuracy.

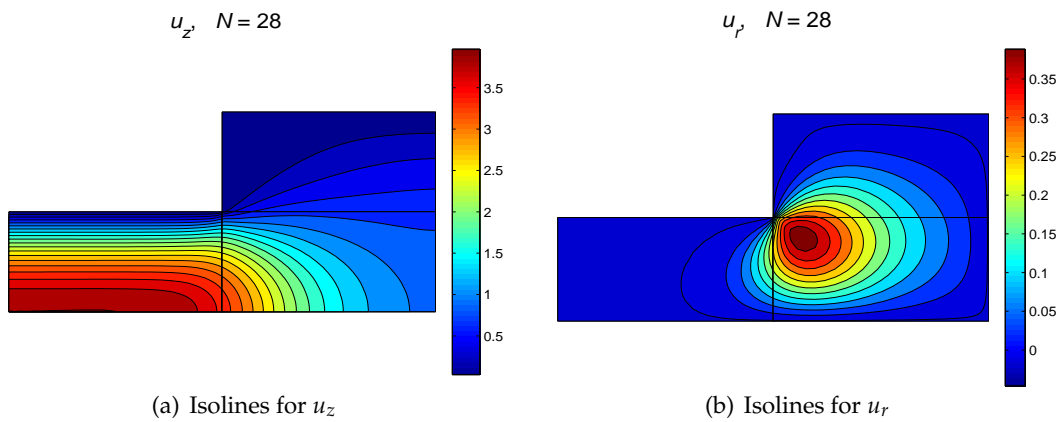


Figure 2: Results for Example 1, $k = 0, N = 28$.

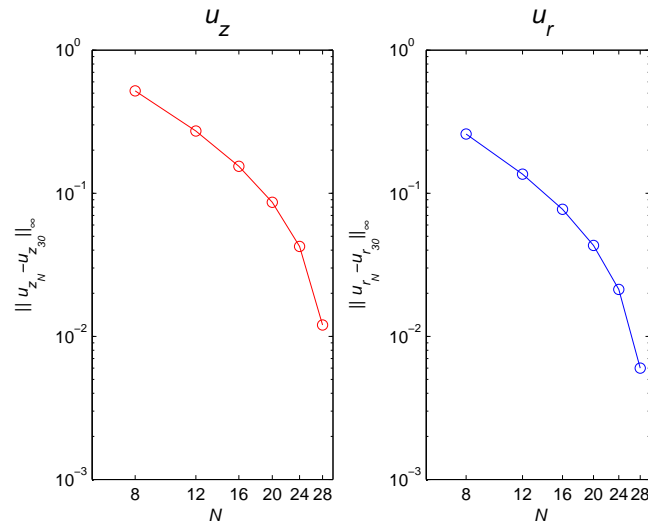


Figure 3: Convergence curves for u_z and u_r for first geometry, $k = 0$.

5.1.2 Case $k = 3$

In Figs. 4(a) and 4(b), we present the isolines of the coordinates u_z and u_θ of the velocity, respectively, for $N = 20$. These results are in excellent agreement with the corresponding results of [2]. The same comments as those mentioned for $k = 0$ regarding the consistency of the figures for values of N as low as 12 also apply in this case.

We also calculated the values of u_z, u_r and u_θ on a uniform 51×51 grid in each of the three elements for $N = 8, 10, 12, 14, 16, 18, 20$ and 22. We subsequently calculated the quantities $\|u_{z_N} - u_{z_{22}}\|_\infty, \|u_{r_N} - u_{r_{22}}\|_\infty, \|u_{\theta_N} - u_{\theta_{22}}\|_\infty, N = 8, 10, 12, 14, 16, 18$ and 20, to be the maximum absolute difference at these points. In Fig. 5, we present the log-log plots for these quantities versus N . All three plots in Fig. 5 exhibit spectral accuracy.

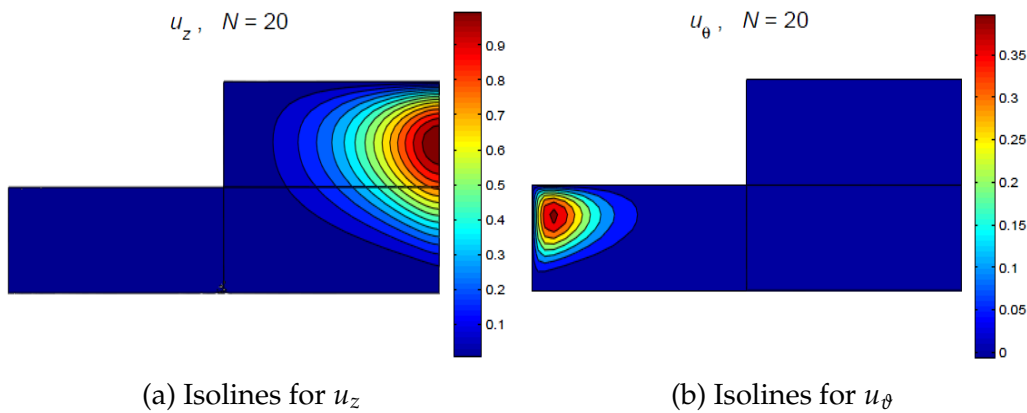


Figure 4: Results for Example 1, $k = 3, N = 20$.

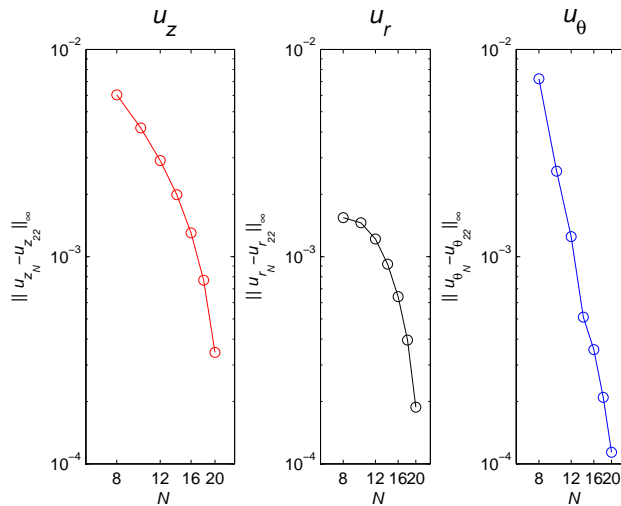


Figure 5: Convergence curves for u_z, u_r and u_θ for first geometry, $k = 3$.

5.2 Example 2

We consider domain depicted in Fig. 6, defined by (in (r, z))

$$\omega_I = [0, 1] \times [-2, 0], \quad \omega_{II} = [0, 1] \times [0, 2],$$

and ω_{III} is the trapezium with vertices $(1, 0), (1, 2), (2, 2)$ and $(3/2, 0)$.

In this example, the element ω_{III} is non-rectangular and the mapping F_{III} is given by (see Remark 3.1)

$$F_{III}(\zeta, \bar{\zeta}) = \begin{pmatrix} \frac{1}{8}[\zeta + 3\bar{\zeta} + \zeta\bar{\zeta} + 11] \\ \bar{\zeta} + 1 \end{pmatrix}.$$

Also, the absolute value of the determinant of the Jacobian is

$$J_{III} = \frac{1}{8}(3 + \bar{\zeta}).$$

In Figs. 7(a) and 7(b), we present the isolines of the coordinates u_z and u_r of the velocity, respectively, for $N = 28$. As in Example 1, the results are consistent for values of N as low as 12.

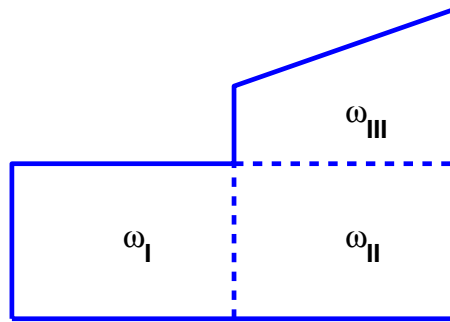


Figure 6: Geometry for Example 2.

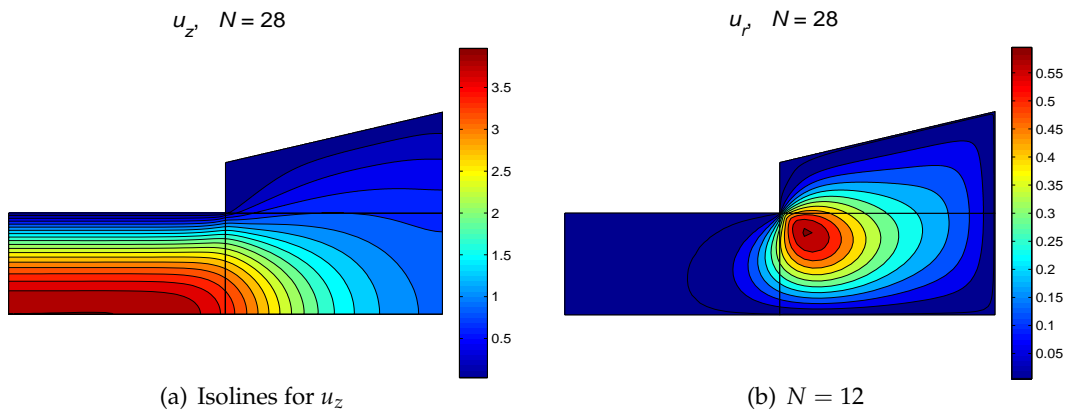


Figure 7: Results for Example 2, $k = 0, N = 28$.

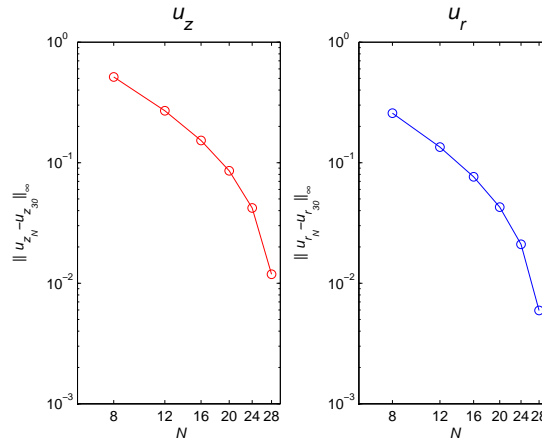


Figure 8: Convergence curves for u_z and u_r for Example 2, $k = 0$.

We also calculated the values of u_z and u_r on a uniform 51×51 grid in each of the three elements for $N = 8, 12, 16, 20, 24, 28$ and 30. We subsequently calculated the quantities $\|u_{z_N} - u_{z_{30}}\|_{\infty}, \|u_{r_N} - u_{r_{30}}\|_{\infty}, N = 8, 12, 16, 20, 24, 28$, to be the maximum absolute difference at these points. In Fig. 8, we present the log-log plots for $\|u_{z_N} - u_{z_{30}}\|_{\infty}$ and $\|u_{r_N} - u_{r_{30}}\|_{\infty}$ versus N . Both plots in Fig. 8 exhibit spectral accuracy.

5.3 Example 3

We consider domain depicted in Fig. 9, defined by (in (r, z))

$$\omega_I = [0, 1] \times [-2, -1], \quad \omega_{III} = [0, 2] \times [0, 2],$$

and ω_{II} is the trapezium with vertices $(0, -1), (0, 1), (2, 1)$ and $(1, -1)$.

In this example, the element ω_{II} is non-rectangular and the mapping F_{II} is given by (see Remark 3.1)

$$F_{II}(\zeta, \xi) = \begin{pmatrix} \frac{1}{4}(\xi + 3)(\zeta + 1) \\ \zeta \end{pmatrix}.$$

Also, the absolute value of the determinant of the Jacobian is

$$J_{II} = \frac{1}{4}(3 + \xi).$$

In Figs. 10(a) and 10(b), we present the isolines of the coordinates u_z and u_r of the velocity, respectively, for $N = 28$. As in Examples 1 and 2, the results are consistent for values of N as low as 12.

We also calculated the values of u_z and u_r on a uniform 51×51 grid in each of the three elements for $N = 8, 12, 16, 20, 24, 28$ and 30. We subsequently calculated the quantities $\|u_{z_N} - u_{z_{30}}\|_{\infty}, \|u_{r_N} - u_{r_{30}}\|_{\infty}, N = 8, 12, 16, 20, 24, 28$, to be the maximum absolute difference at these points. In Fig. 11, we present the log-log plots for $\|u_{z_N} - u_{z_{30}}\|_{\infty}$ and $\|u_{r_N} - u_{r_{30}}\|_{\infty}$ versus N . Both plots in Fig. 11 exhibit spectral accuracy.

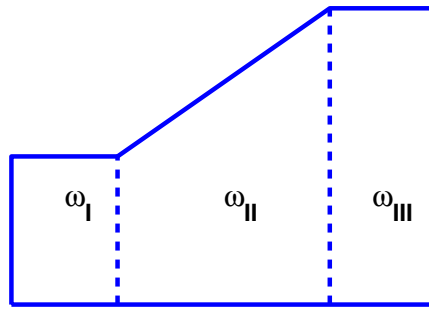


Figure 9: Geometry for Example 3.

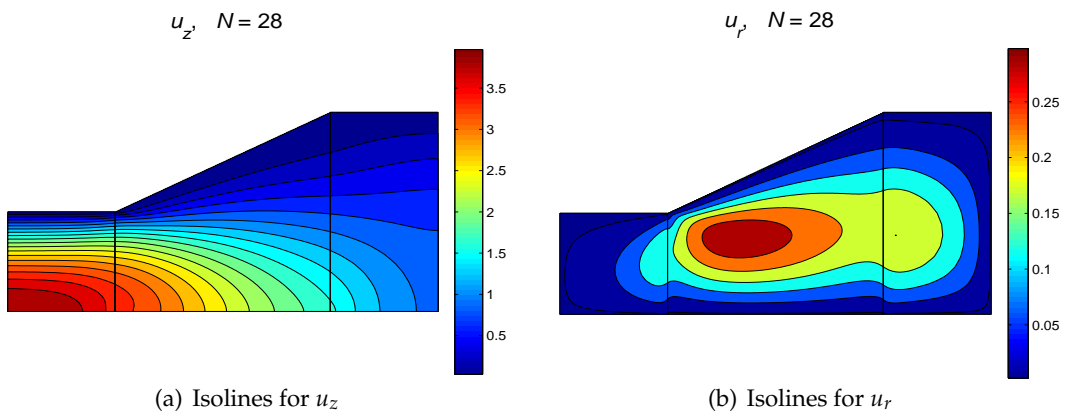


Figure 10: Results for Example 3, $k = 0$, $N = 28$.

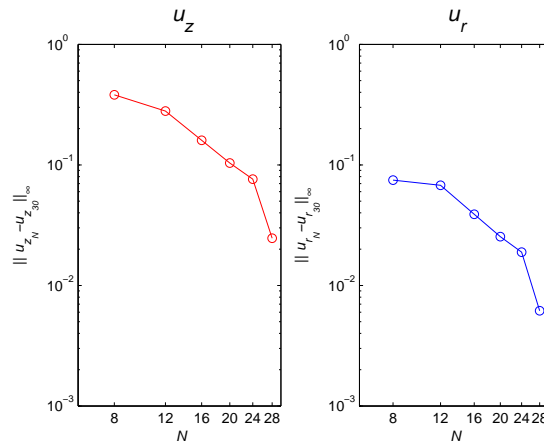


Figure 11: Convergence curves for u_z and u_r for Example 3, $k = 0$.

5.4 Example 4

We consider domain depicted in Fig. 12, defined by (in (r, z))

$$\omega_I = [0, 1] \times [-2, 0], \quad \omega_{II} = [0, 1] \times [0, 2],$$

and ω_{III} is the curvilinear element with vertices $(1,0), (1,2), (2,2)$ and $(3/2,0)$. The segments joining the vertices $(1,0)$ and $(1,2), (1,2)$ and $(2,2)$, and $(2,2)$ and $(3/2,0)$ are all straight lines while the segment joining the vertices $(3/2,0)$ and $(2,2)$ is curved and described by the equation

$$r = \alpha(z) = \frac{3}{2} + \frac{3}{8}z - \frac{1}{16}z^2.$$

In this example, the element ω_{III} is non-rectangular and curved and the mapping F_{III} is given by (see Remark 3.1)

$$F_{III}(\zeta, \xi) = \begin{pmatrix} 1 + \frac{(\zeta+1)(\alpha(\xi+1) - 1)}{\xi+1} \\ \xi+1 \end{pmatrix}.$$

Also, the absolute value of the determinant of the Jacobian is

$$J_{III} = \frac{1}{2}(\alpha(\xi+1) - 1).$$

In Figs. 13(a) and 13(b), we present the isolines of the coordinates u_z and u_r of the velocity, respectively, for $N = 28$. As in the previous examples, the results are consistent for values of N as low as 12.

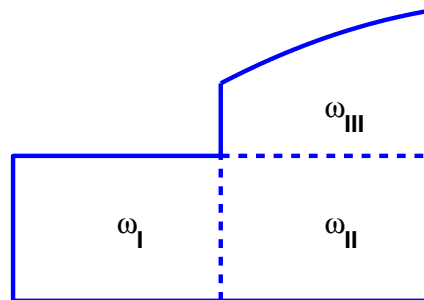


Figure 12: Geometry for Example 4.

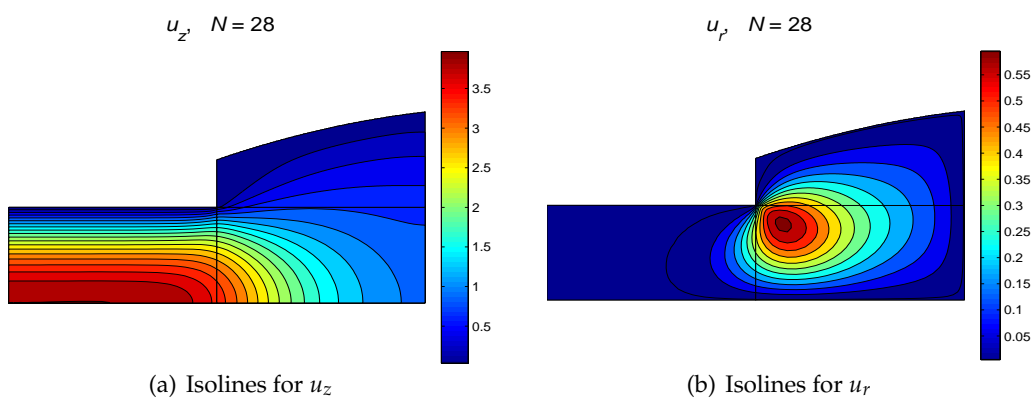


Figure 13: Results for Example 4, $k = 0, N = 28$.

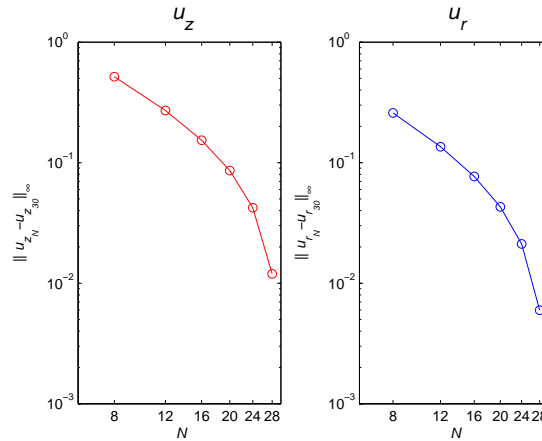


Figure 14: Convergence curves for u_z and u_r for Example 4, $k = 0$.

We also calculated the values of u_z and u_r on a uniform 51×51 grid in each of the three elements for $N = 8, 12, 16, 20, 24, 28$ and 30 . We subsequently calculated the quantities $\|u_{z_N} - u_{z_{30}}\|_{\infty}$, $\|u_{r_N} - u_{r_{30}}\|_{\infty}$, $N = 8, 12, 16, 20, 24, 28$, to be the maximum absolute difference at these points. In Fig. 14, we present the log-log plots for $\|u_{z_N} - u_{z_{30}}\|_{\infty}$ and $\|u_{r_N} - u_{r_{30}}\|_{\infty}$ versus N . Both plots in Fig. 14 exhibit spectral accuracy.

6 Conclusions

In the current study, we investigate the solution of the Stokes equations in deformed axisymmetric geometries. These may include trapezoidal or curved boundaries which are, in general, difficult to treat. By means of truncated Fourier series expansions in the azimuthal direction, the three-dimensional problem is reduced to a series of two-dimensional problems. Each of these problems is subsequently solved numerically by combining the idea of over-integration with the spectral mortar element method. The numerical results of several examples exhibit the expected spectral accuracy and are in excellent agreement with results from the literature.

The extension of the proposed technique to the solution of the Navier-Stokes equations in deformed axisymmetric geometries is a topic of future research.

Appendix

Lagrange interpolating polynomials and their derivatives

We provide information regarding Lagrange interpolating polynomials and their derivatives which is useful in the implementation of the method. For further details see, e.g., [4, 10].

First, recall that the Gauss-Lobatto nodes $\{\xi_j\}_{j=0}^N$ are the zeros of $(1 - \xi^2)L'_N(\xi)$, where $\{L_n\}$ is the set of Legendre polynomials.

On the interval $[-1, 1]$, we define the interpolating polynomials $\{q_j(\zeta)\}_{j=0}^N$ from

$$q_j(\zeta) = -\frac{(1 - \zeta^2) L'_N(\zeta)}{N(N+1)(\zeta - \xi_j) L_N(\xi_j)}, \quad (\text{A.1})$$

and since $L'_N(\xi_i) = 0, i = 1, \dots, N-1$, we have that

$$q_j(\xi_i) = \delta_{ji}, \quad i, j = 0, \dots, N.$$

The first derivatives of the interpolating polynomials are given by

$$q'_j(\zeta) = \frac{1}{L_N(\xi_j)} \frac{L_N(\zeta)}{(\zeta - \xi_j)} + \frac{1}{N(N+1)L_N(\xi_j)} \frac{(1 - \zeta^2) L'_N(\zeta)}{(\zeta - \xi_j)^2}. \quad (\text{A.2})$$

For $j = 1, \dots, N-1$ and $i = 0, \dots, N, i \neq j$, we have

$$q'_j(\xi_i) = \frac{1}{L_N(\xi_j)} \frac{L_N(\xi_i)}{(\xi_i - \xi_j)},$$

while for $j = 1, \dots, N-1$ and $i = j$,

$$q'_j(\xi_j) = \frac{L'_N(\xi_j)}{2L_N(\xi_j)}.$$

Finally, for $i = 0, \dots, N$,

$$q_0(\xi_i) = (-1)^{N-1} \frac{(1 - \xi_i) L''_N(\xi_i) - L'_N(\xi_i)}{N(N+1)},$$

$$q_N(\xi_i) = \frac{(1 + \xi_i) L''_N(\xi_i) + L'_N(\xi_i)}{N(N+1)}.$$

The second derivatives of the interpolating polynomials are given by

$$q''_j(\zeta) = \frac{1}{L_N(\xi_j)} \left(\frac{L'_N(\zeta)}{(\zeta - \xi_j)} - \frac{2L_N(\zeta)}{(\zeta - \xi_j)^2} - \frac{2(1 - \zeta^2) L'_N(\zeta)}{N(N+1)(\zeta - \xi_j)^3} \right). \quad (\text{A.3})$$

For $j = 1, \dots, N-1$ and $i = 0, \dots, N, i \neq j$, we have

$$q''_j(\xi_i) = \frac{1}{L_N(\xi_j)} \left(\frac{L'_N(\xi_i)}{(\xi_i - \xi_j)} - \frac{2L_N(\xi_i)}{(\xi_i - \xi_j)^2} \right),$$

while for $j = 1, \dots, N-1$ and $i = j$,

$$q''_j(\xi_j) = \frac{L''_N(\xi_j)}{3L_N(\xi_j)}.$$

Finally, for $i = 0, \dots, N$,

$$q''_0(\xi_i) = (-1)^{N-1} \frac{(1 - \xi_i) L'''_N(\xi_i) - 2L''_N(\xi_i)}{N(N+1)},$$

$$q''_N(\xi_i) = \frac{(1 + \xi_i) L'''_N(\xi_i) + 2L''_N(\xi_i)}{N(N+1)}.$$

Acknowledgements

The authors would like to thank the University of Cyprus for supporting this research and Professor Christine Bernardi of the C.N.R.S. for her help and suggestions. The authors also wish to thank the two anonymous referees for their constructive comments and helpful suggestions.

References

- [1] G. K. BATCHELOR, *An Introduction to Fluid Dynamics*, Cambridge University Press, Cambridge, 1993.
- [2] Z. BELHACHMI, C. BERNARDI, S. DEPARIS AND F. HECHT, *A truncated Fourier/finite element discretization of the Stokes equations in an axisymmetric domain*, *Math. Models Methods Appl. Sci.*, 16 (2006), pp. 233–263.
- [3] Z. BELHACHMI, C. BERNARDI, S. DEPARIS AND F. HECHT, *An efficient discretization of the Navier-Stokes equations in an axisymmetric domain, part 1: the discrete problem and its numerical analysis*, *J. Sci. Comput.*, 27 (2006), pp. 97–110.
- [4] Z. BELHACHMI, C. BERNARDI AND A. KARAGEORGHIS, *Spectral element discretization of the circular driven cavity, part II: the bilaplacian equation*, *SIAM J. Numer. Anal.*, 38 (2001), pp. 1926–1960.
- [5] Z. BELHACHMI, C. BERNARDI AND A. KARAGEORGHIS, *Spectral element discretization of the circular driven cavity, part III: the Stokes equations in primitive variables*, *J. Math. Fluid. Mech.*, 5 (2003), pp. 24–69.
- [6] Z. BELHACHMI AND A. KARAGEORGHIS, *A spectral mortar element discretization of the Poisson equation with mixed boundary conditions*, *J. Sci. Comput.*, 30 (2007), pp. 275–299.
- [7] Z. BELHACHMI AND A. KARAGEORGHIS, *Spectral element discretization of the Stokes equations in complex geometries: implementational details*, Technical Report TR-06-2009, Department of Mathematics and Statistics, University of Cyprus, 2009.
- [8] F. BEN BELGACEM, *The mortar finite element method with Lagrange multipliers*, *Numer. Math.*, 84 (1999), pp. 173–197.
- [9] C. BERNARDI, M. DAUGE, Y. MADAY AND M. AZAÏEZ, *Spectral Methods for Axisymmetric Domains*, Series in Applied Mathematics 3, Gauthier-Villars & North-Holland, Paris, 1999.
- [10] C. BERNARDI AND Y. MADAY, *Approximations Spectrales de Problèmes aux Limites Elliptiques*, Springer-Verlag, Paris, 1992.
- [11] C. BERNARDI AND Y. MADAY, *Spectral methods*, in *Handbook of Numerical Analysis V*, P. G. Ciarlet and J. -L. Lions eds, North-Holland, pp. 209–485, 1997.
- [12] P. G. CIARLET, *Introduction à l'Analyse Numérique Matricielle et à l'Optimisation*, Collection "Mathématiques Appliquées pour la Maîtrise", Masson, Paris, 1982.
- [13] V. GIRAULT AND P.-A. RAVIART, *Finite Element Methods for Navier-Stokes Equations, Theory and Algorithms*, Springer-Verlag, Berlin, 1986.
- [14] J. -L. LIONS AND E. MAGENES, *Problèmes aux Limites Non Homogènes et Applications*, Dunod, Paris, 1968.
- [15] Y. MADAY AND E. M. RONQUIST, *Optimal error analysis of spectral methods with emphasis on non-constants and deformed geometries*, *Comput. Methods Appl. Mech. Engrg.*, 80 (1990), pp. 91–115.